

# The relevance of $\gamma_L^*$ in hard collisions of virtual photons

Jiří Chýla and Marek Taševský

*Institute of Physics, Na Slovance 2, Prague 8, Czech Republic*

## Abstract

We explore the relevance of extending the concept of the structure to the longitudinally polarized virtual photon involved in hard collisions. We show that for moderate photon virtualities and in the kinematical region accessible in current experiments at HERA and LEP, the contributions of its longitudinal polarization to hard collisions are sizable and should be taken into account as part of the resolved photon component.

## 1 Introduction

In QED quantized in covariant gauge, longitudinally polarized on-shell photons are present, but due to gauge invariance decouple, order by order in perturbation theory, in expressions for physical quantities. For the virtual photon with nonzero virtuality <sup>1</sup> its longitudinal polarization, denoted  $\gamma_L^*$ , does, however, give nonzero contributions to physical quantities and gauge invariance merely requires that these contributions vanish as  $P^2 \rightarrow 0$ . In this paper we discuss hard collisions <sup>2</sup> of virtual photons and, moreover, restrict our attention to kinematical region  $P^2 \ll Q^2$  where the concept of virtual photon structure makes good sense.

This work has been motivated by the lack of the general attitude toward the role of  $\gamma_L^*$  in hard collisions <sup>3</sup> and in particular by our disagreement with the statements of a recent paper [2], where the treatment of virtuality dependence of physical quantities is based on the following two claims <sup>4</sup>

- (i) effects of  $f_{\gamma(P^2)/e}^L$  should be neglected since the corresponding longitudinal cross-sections are suppressed by powers of  $P^2/Q^2$ , and
- (ii) cross-sections of partonic subprocesses involving  $\gamma(P^2)$  should be calculated as if  $P^2 = 0$  due (partly) to the  $P^2/Q^2$  suppression of any additional terms.

In the next Section we first analyze these claims and point out why they are wrong. Then we recall the reasons for introducing the concept of virtual photon structure and recollect basic formulae concerning the structure of  $\gamma_L^*$ . Numerical results illustrating the importance of including the contributions of  $\gamma_L^*$  are presented in Section 3. The feasibility of extracting the information of partonic content of  $\gamma_L^*$  from jet production at HERA is addressed in Section 4, followed by the summary and conclusions in Section 5.

<sup>1</sup>In this paper the virtuality  $\tau$  of a particle with four-momentum  $k$  and mass  $m$  is defined as  $\tau \equiv m^2 - k^2$ . In this convention,  $P^2 > 0$  in the space-like region relevant for hard collisions involving photons in the initial state.

<sup>2</sup>Characterized by some “hard scale” denoted generically as  $Q^2$ . In practice “ $Q^2$ ” may be standard  $Q^2$  in DIS,  $E_T^2$  in jet studies,  $M_Q^2$  in heavy quark production, etc.

<sup>3</sup>The relevance of  $\gamma_L^*$  has recently been pointed out in [1] as well.

<sup>4</sup> $f_{\gamma(P^2)/e}^L$  in the notation of [2] corresponds to  $f_L^\gamma(P^2)$  in our formula (3).

## 2 Theoretical considerations

### 2.1 Virtuality dependence of $\sigma(\gamma_L^*)$

Before recalling practical usefulness of the concept of partonic structure of virtual photons, let us show why the claims made in [2] and mentioned in the Introduction are incorrect. The fact that in the resolved photon channel the cross-sections of  $\gamma_L^*$  are not suppressed by  $P^2/Q^2$  follows directly from analysis of the formula (E.1) in [3] for the cross-section  $\sigma_{TL}$  (denoted  $\sigma_{TS}$  there), which shows that for small  $P^2 \ll m_q^2$  ( $m_q$  being the quark mass) its contribution to  $F_2^\gamma(x, P^2, Q^2)$  behaves as <sup>5</sup>

$$F_{TL}^\gamma(x, P^2, Q^2) = \frac{P^2}{m_q^2} \frac{\alpha}{\pi} 4x^3(1-x)^2 = \frac{P^2}{m_q^2} 2x \frac{\alpha}{2\pi} 4x^2(1-x)^2. \quad (1)$$

This expression coincides, apart from the factor  $N_c e_q^2$  appropriate to a quark with electric charge  $e_q$  and  $N_c$  colors, with the QED expression for distribution function of quarks inside  $\gamma_L^*$  in our formulae (9) below <sup>6</sup> multiplied by  $2x(\alpha/2\pi)$ . For  $P^2 \gg m_q^2$ , on the other hand, the distribution function (8) is proportional to  $4x(1-x)$  with no  $P^2/Q^2$  suppression. As a result, in the region  $P^2 \gg m_q^2$ ,  $\gamma_L^*$  supplies finite contribution to  $F_2^\gamma(x, P^2, Q^2)$  equal to  $(\alpha/\pi)(N_c e_q^2)4x(1-x)$  [4]. Similarly, also the second claim (ii) is incorrect, because also part of the contribution of  $\sigma_{TT}$  has the same  $P^2$  behaviour as in (1). Physical explanation of this behaviour is simple: even for large values of  $Q^2$  the virtuality  $\tau$  of the quarks (antiquarks) from the primary splitting  $\gamma^* \rightarrow q\bar{q}$  of the target photon comes predominantly from the region close to its minimal value  $\tau^{\min} = xP^2 + m_q^2/(1-x)$  and therefore the threshold behaviour is governed by the quark mass  $m_q$  rather than  $Q^2$ .

On the other hand, virtuality dependence of the contributions of  $\gamma_T^*$  and  $\gamma_L^*$  can be safely neglected in the LO direct photon hard processes, for instance in large  $E_T$  jet production via the photon-gluon fusion subprocess  $\gamma^* G \rightarrow q\bar{q}$ . In these processes virtuality of the exchanged quark (or antiquark) is forced by kinematics to be proportional to jet transverse energy  $E_T$  and therefore the virtuality dependent part is suppressed by powers of  $P^2/E_T^2$ . Of course, in realistic QCD the onset of quark distribution functions of  $\gamma_L^*$  is not expected to be determined directly by quark masses, but rather by some nonperturbative parameter related to confinement, but the basic features of the dependence on  $P^2$ , exemplified in (1), are likely to persist.

### 2.2 Equivalent photon approximation

Most of the present knowledge of the structure of the photon comes from experiments at the ep and  $e^+e^-$  colliders, where the incoming leptons act as sources of transverse and longitudinal virtual photons. To order  $\alpha$  their respective unintegrated fluxes are given as

$$f_T^\gamma(y, P^2) = \frac{\alpha}{2\pi} \left( \frac{1 + (1-y)^2}{y} \frac{1}{P^2} - \frac{2m_e^2 y}{P^4} \right), \quad (2)$$

$$f_L^\gamma(y, P^2) = \frac{\alpha}{2\pi} \frac{2(1-y)}{y} \frac{1}{P^2}. \quad (3)$$

Phenomenological analyses of interactions of virtual photons have so far concentrated on its transverse polarization. The same holds for available parameterizations of parton distribution functions (PDF) of virtual photons. Neglecting longitudinal photons is in general a good approximation for

<sup>5</sup>In the notation of [3] the first and second subscripts in  $\sigma_{ij}$  refer to polarizations of the probing and target photons respectively, with virtualities  $Q^2$  and  $P^2$ . Most of the terms in the expression for  $\sigma_{TL}$  do, indeed, behave as  $P^2/Q^2$ , but there is one, proportional to  $(\Delta t q_1^4/T)$ , which does not and which yields (1).

<sup>6</sup>In practical applications the factorization scale  $M^2$  in (5) is identified with the generic hard scale  $Q^2$ .

$y \rightarrow 1$ , where the flux  $f_L^\gamma(y, P^2) \rightarrow 0$ , as well as for very small virtualities  $P^2$ , where PDF of  $\gamma_L^*$  vanish by gauge invariance. But how small is “very small” in fact? For instance, should we take into account the contribution of  $\gamma_L^*$  to jet cross-section in the region  $E_T \gtrsim 5$  GeV,  $P^2 \gtrsim 1$  GeV<sup>2</sup>, where most of the data on virtual photons obtained in ep collisions at HERA come from? The rest of this paper is devoted to addressing this and related questions.

### 2.3 Who needs the concept of partonic structure of virtual photons?

Let us briefly recall the virtue of extending the concept of partonic “structure” to virtual photons. The arguments for it were discussed in detail in [5–7] and we therefore merely summarize the most important points:

- In principle, the concept of partonic structure of (sufficiently) virtual photons can be dispensed with because higher order perturbative QCD corrections to cross-sections of processes involving virtual photons in the initial state are well-defined and finite even for massless partons.
- In practice, however, this concept is extraordinarily useful as it allows us to include the resummation of higher order QCD effects that come from physically well-understood region of (almost) parallel emission of partons off the quark (or antiquark) coming from the primary  $\gamma^* \rightarrow q\bar{q}$  splitting and subsequently participating in hard processes.

In other words, for the virtual photon, as opposed to the real one, its PDF can be regarded as “merely” describing higher order perturbative effects and not the “true” structure. Although this distinction between the content of PDF of real and virtual photons does exist, it does not affect the extraordinary *phenomenological* usefulness of PDF of the virtual photon. As shown in [5–7] the non-trivial part of the resolved photon contributions to NLO calculations of dijet production at HERA obtained with JETVIP [8] is large and affects significantly the conclusions of phenomenological analyses of existing experimental data.

### 2.4 Structure of $\gamma_L^*$ in QED

The definition and evaluation of quark distribution functions of the virtual photon in QED serves as a guide to QCD improved parton model predictions of virtuality dependence of their pointlike parts. In pure QED and to order  $\alpha$  the probability of finding inside  $\gamma_T^*$  or  $\gamma_L^*$  of virtuality  $P^2$  a quark with mass  $m_q$ , electric charge  $e_q$ , momentum fraction  $x$  and virtuality  $\tau \leq M^2$ , is given, in units of  $3e_q^2\alpha/2\pi$ , as [7] ( $k = T, L$ )

$$q_k^{\text{QED}}(x, m_q^2, P^2, M^2) = f_k(x) \ln \left( \frac{M^2}{\tau^{\min}} \right) + \left[ -f_k(x) + \frac{g_k(x)m_q^2 + h_k(x)P^2}{\tau^{\min}} \right] \left( 1 - \frac{\tau^{\min}}{M^2} \right), \quad (4)$$

where  $\tau^{\min} = xP^2 + m_q^2/(1-x)$ . The quantity defined in (4) has a clear physical interpretation: it describes the flux of quarks and antiquarks that are almost collinear with the incoming photon and “live” longer <sup>7</sup> than  $1/M$ . For  $\tau^{\min} \ll M^2$  the expression (4) simplifies to

$$q_k^{\text{QED}}(x, m_q^2, P^2, M^2) = f_k(x) \ln \left( \frac{M^2}{xP^2 + m_q^2/(1-x)} \right) - f_k(x) + \frac{g_k(x)m_q^2 + h_k(x)P^2}{xP^2 + m_q^2/(1-x)}, \quad (5)$$

which for  $x(1-x)P^2 \gg m_q^2$  reduces further to

$$q_k^{\text{QED}}(x, 0, P^2, M^2) = f_k(x) \ln \left( \frac{M^2}{xP^2} \right) - f_k(x) + \frac{h_k(x)}{x}. \quad (6)$$

---

<sup>7</sup>In fact most of these quarks live much longer than  $1/M$ .

The functions  $f_k, g_k, h_k$  are given as [7]

$$\begin{aligned} f_T(x) &= x^2 + (1-x)^2, & g_T(x) &= \frac{1}{1-x}, & h_T(x) &= 0, \\ f_L(x) &= 0, & g_L(x) &= 0, & h_L(x) &= 4x^2(1-x). \end{aligned} \quad (7)$$

For  $M^2 \gg x(1-x)P^2$  the quark distribution function of  $\gamma_L^*$  has a simple form

$$q_L^{\text{QED}}(x, m_q^2, P^2, M^2) = \frac{4x^2(1-x)^2 P^2}{x(1-x)P^2 + m_q^2} \rightarrow 4x(1-x); \quad x(1-x)P^2 \gg m_q^2 \quad (8)$$

$$\rightarrow \frac{P^2}{m_q^2} 4x^2(1-x)^2; \quad x(1-x)P^2 \ll m_q^2 \quad (9)$$

## 2.5 QCD corrections

For  $\gamma_T^*$  QCD corrections to QED formula (6) are well understood. Though important, in particular for large and very small  $x$ , they do not change its basic features and the main nontrivial effect comes from the emergence of gluons inside  $\gamma_T^*$ . For  $\gamma_L^*$  the effects of collinear parton radiation off the quarks/antiquarks from the  $\gamma_L^* \rightarrow q\bar{q}$  splitting result in factorization scale dependence that resembles those of hadrons and will be discussed in separate paper. For the purpose of this exploratory study we use the QED formula (8) throughout this paper.

## 3 Numerical results

### 3.1 DIS on $\gamma^*$ in QED

The cleanest evidence of the importance of taking into account the contribution of  $\gamma_L^*$  has been provided by the L3 and OPAL measurements [9, 10] of the QED structure function  $F_2^{\gamma, \text{QED}}$  at LEP. In these measurements, based on the analysis of  $\mu^+\mu^-$  final states, the average target photon virtuality is small ( $\langle P^2 \rangle = 0.033 \text{ GeV}^2$  in [9] and  $\langle P^2 \rangle = 0.05 \text{ GeV}^2$  in [10]) but still sufficiently large with respect to  $m_\mu^2 \doteq 0.01 \text{ GeV}^2$  to see the decrease of  $F_2^{\gamma, \text{QED}}(x, P^2, Q^2)$  with respect to the QED prediction for the real photon. To order  $\alpha$  these predictions were calculated exactly in [3] and contain contributions of both transverse and longitudinal polarizations of the target photon. In the region  $m_e^2 \ll P^2 \ll Q^2$  experiments at LEP actually measure the following sum of  $\gamma^*\gamma^*$  cross-sections, the first and second indices corresponding to probe and target photon respectively,

$$F_{\text{eff}}^\gamma(x, P^2, Q^2) \equiv \frac{Q^2}{4\pi^2\alpha} (\sigma_{TT} + \sigma_{LT} + \sigma_{TL} + \sigma_{LL}) = \frac{Q^2}{4\pi^2\alpha} \sigma(P^2, Q^2, W^2), \quad (10)$$

where all cross-sections  $\sigma_{jk}$  are functions of  $W^2, P^2$  and  $Q^2$  and  $x = Q^2/(W^2 + Q^2 + P^2)$ . As shown in [9, 10] the data are in very good agreement with QED prediction for (10) provided the dependence on target photon virtuality  $P^2$  is taken into account. For OPAL kinematical region the QED predictions for  $f(x, P^2, Q^2) \equiv (2\pi/\alpha)F_{\text{eff}}^\gamma(x, P^2, Q^2)$  as well as the individual contributions  $f_{ij}$ , are shown in Fig. 1a, together with the results (shown as dotted curves) corresponding to the real photon and the approximations using formulae of the preceding Section (dashed curves). The variations of  $f_{jk}(x, P^2, Q^2)$  and  $f(x, P^2, Q^2)$  with respect to real photon, defined as ( $i, j = T, L$ )

$$\Delta f_{jk}(x, P^2, Q^2) \equiv f_{jk}(x, P^2, Q^2) - f_{jk}(x, 0, Q^2), \quad (11)$$

are plotted in Fig. 1b. The contribution  $\Delta f_{TL} = f_{TL}$  to the variation  $\Delta F_{\text{eff}}^\gamma(x, P^2, Q^2)$  coming from target  $\gamma_L^*$  is clearly comparable in magnitude to  $\Delta f_{TT}$  and  $\Delta f_{LT}$  coming from target  $\gamma_T^*$ . Neglecting  $\Delta f_{TL}$  would thus lead to serious disagreement between QED predictions and data.

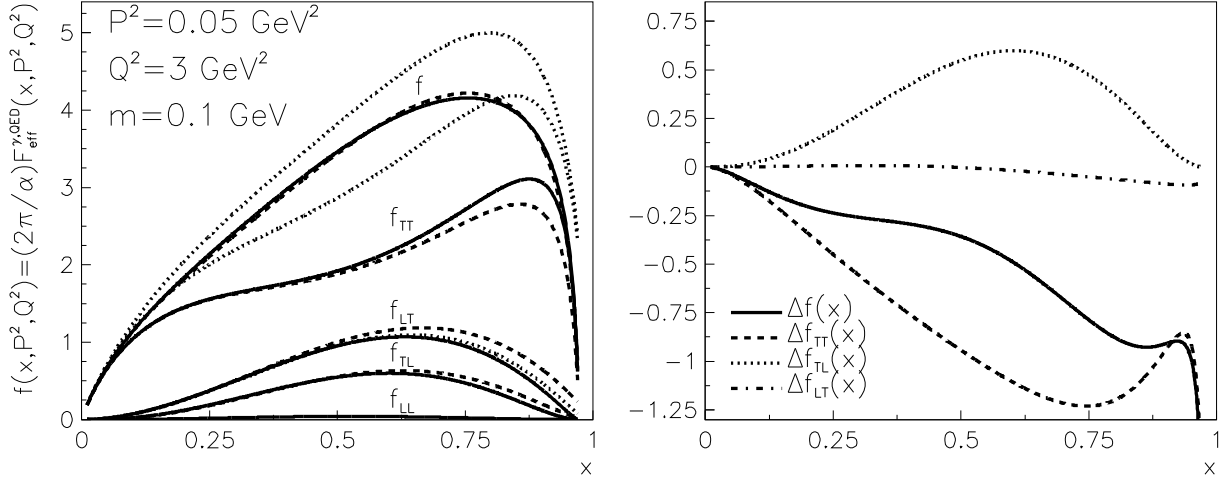


Figure 1: a)  $(2\pi/\alpha)F_{\text{eff}}^{\gamma,\text{QED}}(x, P^2, Q^2)$  evaluated from eq. (10) with  $\sigma_{jk}$  given by exact QED formulae (E.1) of [3] (upper solid curve), together with contributions of individual channels  $\sigma_{jk}$  (other solid curves). The approximate expressions based on the formula (5) as well as the exact ones corresponding to  $P^2 = 0$  are shown as dashed and dotted curves, respectively. b) The corresponding differences  $\Delta f(x, P^2, Q^2)$  and  $\Delta f_{jk}(x, P^2, Q^2)$ .

### 3.2 DIS on $\gamma^*$ in QCD

In LO QCD the structure function  $F_2^\gamma$  is given in terms of quark distribution functions by the same expression as for hadrons<sup>8</sup>

$$F_2^\gamma(x, P^2, Q^2) = \sum_i 2xe_i^2 (q_i(x, P^2, Q^2) + \bar{q}_i(x, P^2, Q^2)). \quad (12)$$

In all existing phenomenological analyses of experimental data only target  $\gamma_T^*$  has been taken into account and to the best of our knowledge no attempt has been made to extract PDF of  $\gamma_L^*$  therefrom. In this exploratory study we compare the results for  $F_2^\gamma$  obtained with Schuler–Sjöstrand (SaS) parameterization [12] of  $q_T(x, P^2, M^2)$  with the QED prediction (8) for  $q_L(x, P^2, M^2)$ .

In Fig. 2 this comparison is performed for typical values of  $P^2$  and  $Q^2$  accessible at LEP and  $m_q^2 = 1, 0.1 \text{ GeV}^2$  and  $m_q^2 = 0$ . The importance of the contributions of  $\gamma_L^*$  with respect to those of  $\gamma_T^*$  depends sensitively on the value of  $m_q$ : whereas for  $m_q \doteq 1 \text{ GeV}$ ,  $\gamma_L^*$  is largely irrelevant, for  $m_q \lesssim 0.3 \text{ GeV}$ , medium values of  $x$  and  $Q^2 \lesssim 100 \text{ GeV}^2$ , its contributions in the considered region of  $P^2$  and  $Q^2$  are comparable to those of SaS1D parameterization of  $\gamma_T^*$ . Only for very large  $Q^2$  does  $\gamma_L^*$  become really negligible with respect to  $\gamma_T^*$ . For fixed  $Q^2$  the relative importance of  $\gamma_L^*$  with respect to  $\gamma_T^*$  grows with  $P^2$ , but to retain clear physical meaning of PDF we stay throughout this paper in the region where  $P^2 \ll Q^2$ .

The comparison of the contributions of  $\gamma_L^*$  and  $\gamma_T^*$  at the same values of  $P^2$  is one measure of the relevance of  $\gamma_L^*$ . If we are interested in virtuality dependence of  $F_2^\gamma(x, P^2, Q^2)$ , the appropriate comparison is with difference

$$\Delta F_2^{\gamma T}(x, P^2, Q^2) \equiv F_2^{\gamma T}(x, 0, Q^2) - F_2^{\gamma T}(x, P^2, Q^2), \quad (13)$$

<sup>8</sup>In the present paper we disregard the consequences of the reformulation of QCD analysis of  $F_2^\gamma$  proposed in [11] as they do not concern the main point of our discussion.

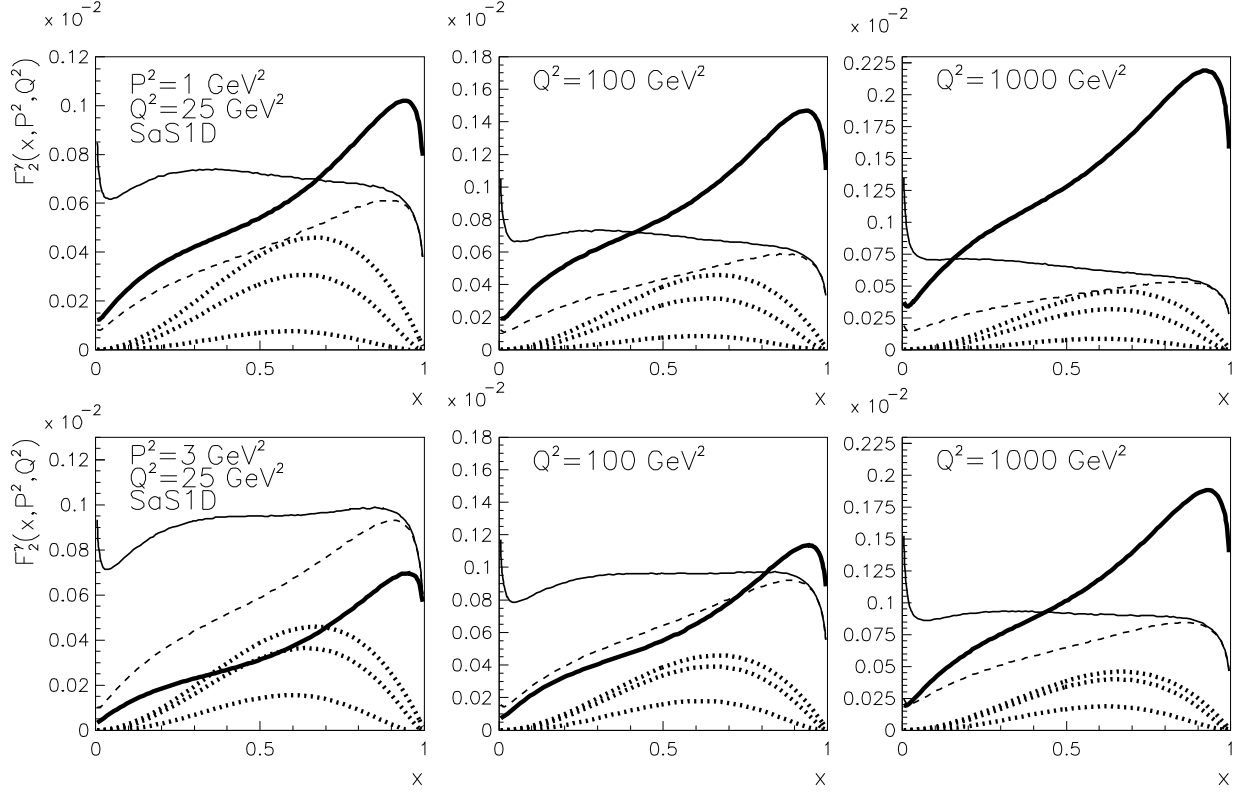


Figure 2: SaS1D parameterization of  $F_2^\gamma(x, P^2, Q^2)$  (thick solid curves) compared to QED formula (8) for, from above,  $m^2 = 0, 0.1$  and  $1 \text{ GeV}^2$  (thick dotted curves). The thin solid curves correspond to  $\Delta F_2^{\gamma T}(x, P^2, Q^2)$ , the dashed ones to the difference (13) of pointlike parts of  $\gamma_T^*$ .

of SaS results for  $\gamma_T^*$ , denoted in Fig. 2 by thin solid curves. At small to moderate  $x$ , lower hard scales  $Q^2$  and larger virtualities  $P^2$ , the contributions of  $\gamma_L^*$  appear by this measure less important than when compared to  $F_2^\gamma(x, P^2, Q^2)$  itself. However, this is due largely to the fact that  $F_2^\gamma$  of the real photon gets a large contribution from its VDM component, whereas the parameterization of  $q_L$  used in this comparison corresponds to purely pointlike expression (8). Compared to the difference (13) of the pointlike parts of  $\gamma_T^*$  only, denoted by dashed curves in Fig. 2, the contributions of  $\gamma_L^*$  are, at least for  $m_q \lesssim 0.3 \text{ GeV}$ , again quite significant throughout large part of the kinematical range considered.

### 3.3 LO calculations of dijet production in ep and $e^+e^-$ collisions

The measurement of dijet production in ep and  $e^+e^-$  collisions provides another way of investigating interactions of the virtual photon [13,14]. In general the cross-sections for dijet production are given as sums of contributions of all possible parton level subprocess. To demonstrate the importance of including the contributions of target  $\gamma_L^*$  it is, however, sufficient to use the approximation of the single effective subprocess [15] in which dijet cross-sections are expressed in terms of the so called *effective parton distribution function* of the target photon

$$D_{\text{eff}}(x, P^2, M^2) \equiv \sum_{i=1}^{n_f} (q_i(x, P^2, M^2) + \bar{q}_i(x, P^2, M^2)) + \frac{9}{4}G(x, P^2, M^2). \quad (14)$$

In Fig. 3 we perform for this quantity the same comparisons as we did in Fig. 2 for  $F_2^\gamma$ , including the comparison with the difference  $\Delta D_{\text{eff}}(x, P^2, Q^2)$ , defined analogously to (13). The fact that in

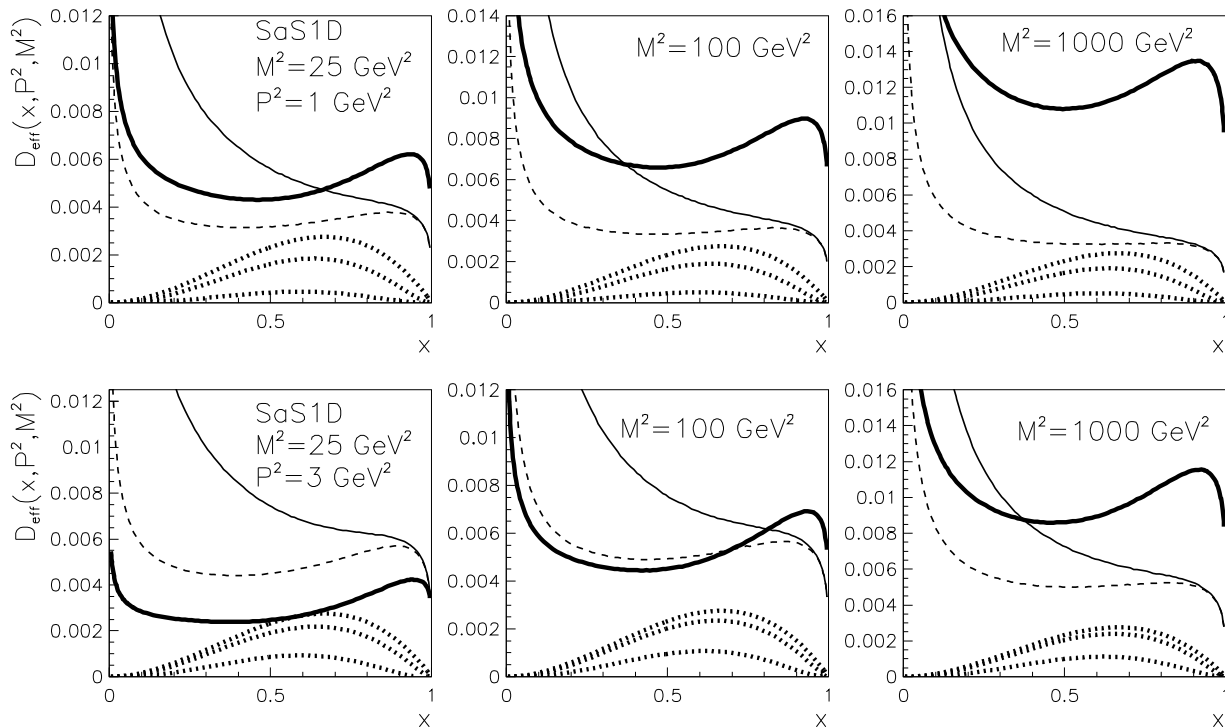


Figure 3: The same as in Fig. 2 but for the quantity  $D_{\text{eff}}(x, P^2, M^2)$  defined in (14).

QED  $\gamma_L^*$  contains no gluons is reflected in substantially smaller relative importance of  $\gamma_L^*$  for  $D_{\text{eff}}$  at small values of  $x$ . Otherwise, however, the messages of Figs. 2 and 3 are the same: in hard processes the relative importance of the contributions of target  $\gamma_L^*$  with respect to those of  $\gamma_T^*$

- depends sensitively on the value of  $m_q$ ,
- peaks around  $x \doteq 0.6$  and vanishes for  $x \rightarrow 0$  and  $x \rightarrow 1$ ,
- grows with target photon virtuality  $P^2$  and
- decreases with factorization scale  $M^2$ .

For physically reasonable value  $m_q = 0.3$  GeV, Figs. 2 and 3 suggest that at least in part of the kinematical range accessible at HERA  $\gamma_L^*$  should definitely be taken into account.

### 3.4 NLO calculations of dijet production in ep collisions

In the preceding subsections we have discussed the importance of including the contributions of  $\gamma_L^*$  to QED or the LO QCD quantities  $F_{\text{eff}}$ ,  $F_2^\gamma$  and  $D_{\text{eff}}$ . In this subsection we shall address the same question within the NLO QCD parton level calculations of dijet cross-sections in ep collisions, obtained with JETVIP [8], currently the only NLO parton level MC program that includes both direct and resolved photon contributions<sup>9</sup>. JETVIP contains the full set of partonic cross-sections for the direct photon contribution up to the order  $\alpha_s^2$ . Examples of such diagrams are in Fig. 4a ( $\alpha_s$  tree diagram) and Fig. 4b ( $\alpha_s^2$  tree diagram). To go one order of  $\alpha_s$  higher and perform

<sup>9</sup>In specifying the powers of  $\alpha$  corresponding to various diagrams we discard one common power of  $\alpha$  coming from the vertex where the incoming electron emits the virtual photon. This vertex is also left out in diagrams of Fig. 4

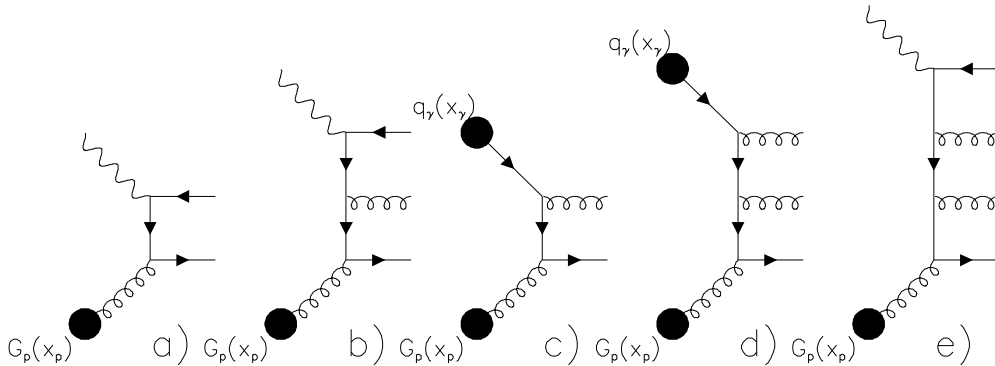


Figure 4: Examples of diagrams contributing to dijet production in ep collisions at the orders  $\alpha\alpha_s$  (a),  $\alpha\alpha_s^2$  (b,c), and  $\alpha\alpha_s^3$  (d,e) taking into account that the upper blobs representing quark distribution functions of the photon are proportional to  $\alpha$ .

complete calculation of the direct photon contributions up to order  $\alpha\alpha_s^3$  would require evaluating tree diagrams like that in Fig. 4e, as well as one-loop corrections to diagrams like in Fig. 4b and two-loop corrections to diagrams like in Fig. 4a. So far, such calculations are not available. In addition to complete  $O(\alpha\alpha_s^2)$  direct photon contribution JETVIP includes also the resolved photon one with partonic cross-sections up to the order  $\alpha_s^3$ , exemplified by diagrams in Fig. 4c,d. The justification for including in the resolved channel terms of the order  $\alpha_s^3$  are discussed in detail in [5–7]. Once the concept of virtual photon structure is introduced, part of the direct photon contribution (which for the virtual photon is actually nonsingular) is subtracted and included in the definition of PDF appearing in the resolved photon contribution. For  $\gamma_T^*$  the subtracted term is given as the convolution of the splitting function <sup>10</sup>

$$q_T^{\text{split}}(x, P^2, M^2) = q_T^{\text{QED}}(x, P^2, Q^2) = \frac{\alpha}{2\pi} 3e_q^2 (x^2 + (1-x)^2) \ln \frac{M^2}{xP^2}. \quad (15)$$

with  $\alpha_s^2$  partonic cross-sections. To avoid misunderstanding we shall henceforth use the term “direct unsubtracted” ( $\text{DIR}_{\text{uns}}$ ) to denote NLO direct photon contributions *before* this subtraction and reserve the term “direct” for the results *after* it. In this terminology the complete JETVIP calculations are given by the sum of direct and resolved parts and denoted  $\text{DIR}+\text{RES}$ . In JETVIP only the terms defining quark distribution function of the transverse virtual photon are subtracted from  $\text{DIR}_{\text{uns}}$  calculations.

In [5–7] we discussed dijet cross-sections calculated by means of JETVIP in the kinematical region typical for HERA experiments

$$E_T^{(1)} \geq E_T^c + \Delta, \quad E_T^{(2)} \geq E_T^c, \quad E_T^c = 5 \text{ GeV}, \quad \Delta = 2 \text{ GeV}$$

$$-2.5 \leq \eta^{(i)} \leq 0, \quad i = 1, 2,$$

in four windows of photon virtuality

$$1.4 \leq P^2 \leq 2.4 \text{ GeV}^2; \quad 2.4 \leq P^2 \leq 4.4 \text{ GeV}^2; \quad 4.4 \leq P^2 \leq 10 \text{ GeV}^2; \quad 10 \leq P^2 \leq 25 \text{ GeV}^2$$

and for  $0.25 \leq y \leq 0.7$ . The whole analysis has been performed in  $\gamma^*p$  CMS. The cuts on  $E_T$  were chosen in such a way that in all  $P^2$  windows  $\langle P^2 \rangle \ll E_T^2$ , thereby ensuring that the virtual

<sup>10</sup>JETVIP works with massless quarks and includes in (15) additional function of  $x$ .



photon lives long enough for its “structure” to develop before the hard scattering takes place. The asymmetric cut in  $E_T$  is appropriate for our decision to plot the sums of  $E_T$  and  $\eta$  distributions of the jets with highest and second highest  $E_T$ . In JETVIP jets are defined by means of the standard cone algorithm with jet momenta defined using the  $E_T$ -weighting recombination procedure and supplemented with the  $R_{\text{sep}}$  parameter. All calculations presented below correspond to  $R_{\text{sep}} = 2$  and were obtained setting the renormalization scale  $\mu$  as well as the factorization scale  $M$  equal to jet transverse energy. The sensitivity to these parameters as well as other ambiguities are discussed in detail in [7, 14].

Beside the splitting term (15), which generates quark distribution function of  $\gamma_T^*$ , one can subtract from NLO direct photon calculations also the integral over the term proportional to  $h_L(x)$  and put it into the definition of quark distribution function of  $\gamma_L^*$ . To do that properly would, however, require modifying the original code in order to take into account different  $y$  dependence of the fluxes of  $\gamma_T^*$  and  $\gamma_L^*$  in (2-3). In this exploratory study we neglect this difference and fake the contributions of  $\gamma_L^*$  simply by running JETVIP in the resolved photon channel using (8) with  $m_q = 0$  as the input PDF. As in the considered region  $\langle y \rangle \doteq 0.4$ , the error incurred by this approximation does not exceed 16%.

But does it make any sense to introduce the concept of PDF of  $\gamma_L^*$ ? Admittedly, for interactions of virtual photons we can stay solely within the framework of  $\text{DIR}_{\text{uns}}$  calculations and thus dispense with the concept of PDF of virtual photons at all. On the other hand, as argued in [5–7], the effects incorporated in the transverse part of resolved photon component of JETVIP are numerically large. In particular, we have emphasized the importance of including in the resolved photon component of JETVIP the  $\alpha_s^3$  partonic cross-sections. These are not included in exact  $\alpha\alpha_s^2$   $\text{DIR}_{\text{uns}}$  calculations and in part of accessible kinematical range more than double the resolved photon contribution to dijet production at HERA compared to the contribution of the  $\alpha_s^2$  partonic cross-sections.

The same effect can be expected for  $\gamma_L^*$  as the NLO  $\text{DIR}_{\text{uns}}$  calculations contain at the order  $\alpha\alpha_s^2$  exact matrix elements which include both transverse and longitudinal polarization of the target photon. To illustrate the importance of including the effects of  $\gamma_L^*$  we compare in Fig. 5 the convolutions  $q_L^{\text{QED}} \otimes \sigma(\alpha_s^2)$  and  $q_L^{\text{QED}} \otimes \sigma(\alpha_s^3)$  with the convolution  $q_T^{\text{QED}} \otimes \sigma(\alpha_s^2)$ . In addition, we overlay the complete NLO  $\text{DIR}+\text{RES}$  and  $\text{DIR}_{\text{uns}}$  results, from which, however, the LO direct photon contribution has been subtracted. Fig. 5 shows that the contributions of  $\gamma_L^*$ , though smaller, are nevertheless comparable to those of  $\gamma_T^*$ , in particular for  $\eta$  close to  $\eta \simeq 0$ . Moreover, in the region  $\eta \gtrsim -1.75$  the sum of the contributions  $(q_T^{\text{QED}} + q_L^{\text{QED}}) \otimes \sigma(\alpha_s^2)$  approximates remarkably well the exact  $\alpha\alpha_s^2$   $\text{DIR}_{\text{uns}}$  calculations. The excess of the exact results over this sum in the region  $\eta \lesssim -1.75$  is primarily due to the fact that the  $\alpha\alpha_s^2$   $\text{DIR}_{\text{uns}}$  calculations contain beside the tree level diagrams describing the production of three final state partons, also one loop corrections to two parton final states, which contribute predominantly at large negative  $\eta$ .

The message of Fig. 5 is quantified by plotting in Fig. 6 the ratios

$$r_k(\eta, P^2) \equiv \frac{q_k^{\text{QED}} \otimes \sigma^{\text{res}}(\alpha_s^2)}{\sigma_{\text{uns}}^{\text{DIR}}(\alpha\alpha_s^2)}, \quad k = T, L \quad (16)$$

of the contributions of  $\gamma_T^*$  and  $\gamma_L^*$ , as well as their sum, to the  $\alpha\alpha_s^2$  part of the  $\text{DIR}_{\text{uns}}$  results. The ratio of the contributions of  $\gamma_L^*$  and  $\gamma_T^*$  is above 1/4 throughout the considered  $\eta$  range and above 1/2 in the region  $\eta \simeq 0$ . Within the  $\text{DIR}_{\text{uns}}$  calculations at the order  $\alpha\alpha_s^2$  in the kinematical region relevant for HERA,  $\gamma_L^*$  is thus comparable in importance to  $\gamma_T^*$ .

The preceding discussion illustrates the importance of the contributions of  $\gamma_L^*$ , but as the  $\alpha\alpha_s^2$   $\text{DIR}_{\text{uns}}$  calculations include them exactly, the genuine nontrivial effect of introducing the concept of PDF of  $\gamma_L^*$  is given in Fig. 5 by the thin dashed-dotted curves, denoting the convolutions

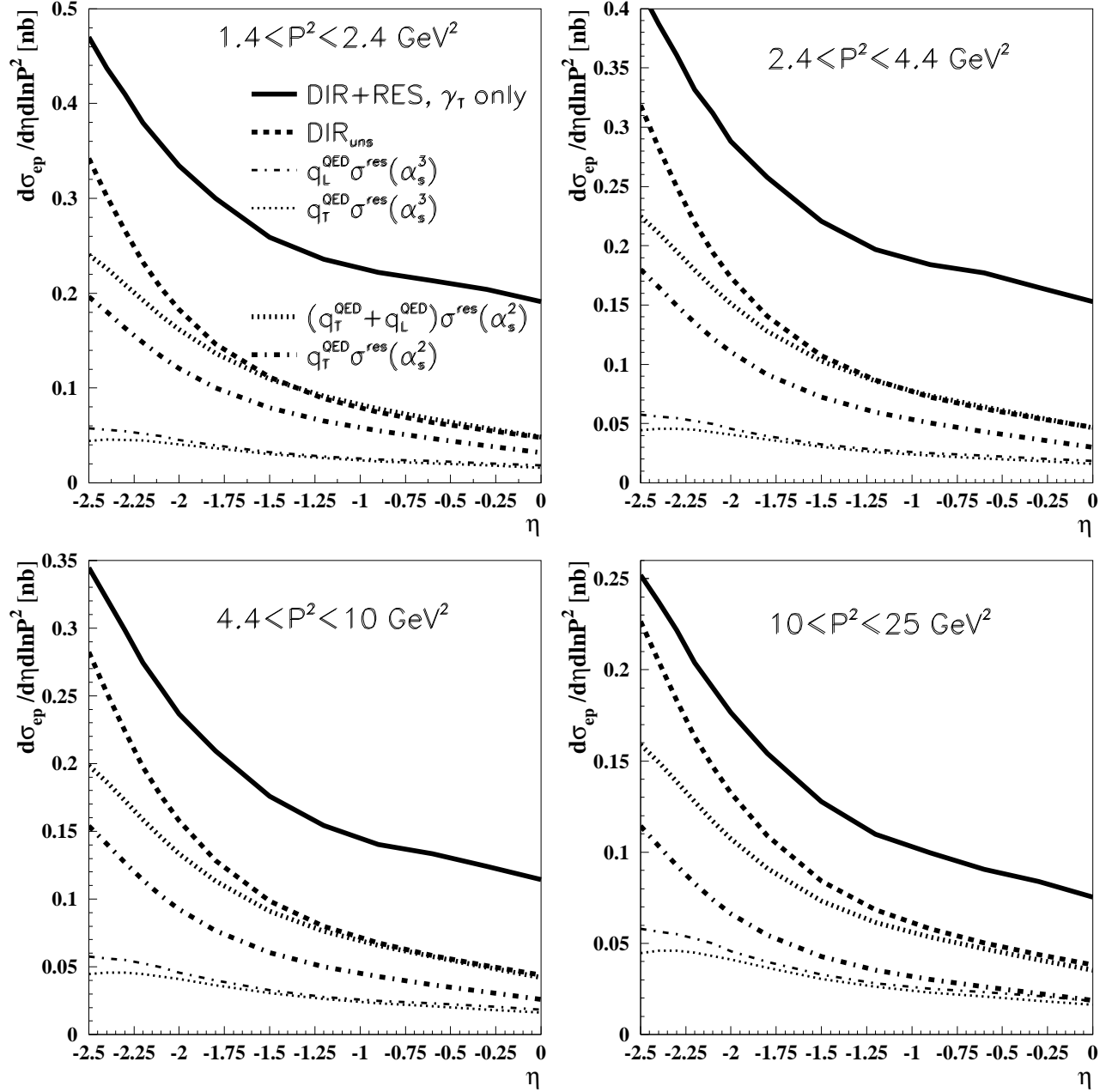


Figure 5: Comparison of the complete JETVIP results taking into account only  $\gamma_T^*$  in the resolved channel with the  $\text{DIR}_{\text{uns}}$  ones and the convolutions of QED expressions  $q_T^{\text{QED}}$  and  $q_L^{\text{QED}}$  with  $\alpha_s^2$  partonic cross-sections. The nontrivial effect of including  $\gamma_L^*$  in the resolved channel, given by the convolution  $q_L^{\text{QED}} \otimes \sigma(\alpha_s^3)$  is shown by thin dash-dotted curves. In the case of  $\text{DIR}+\text{RES}$  and  $\text{DIR}_{\text{uns}}$  results the LO direct contribution has been subtracted.

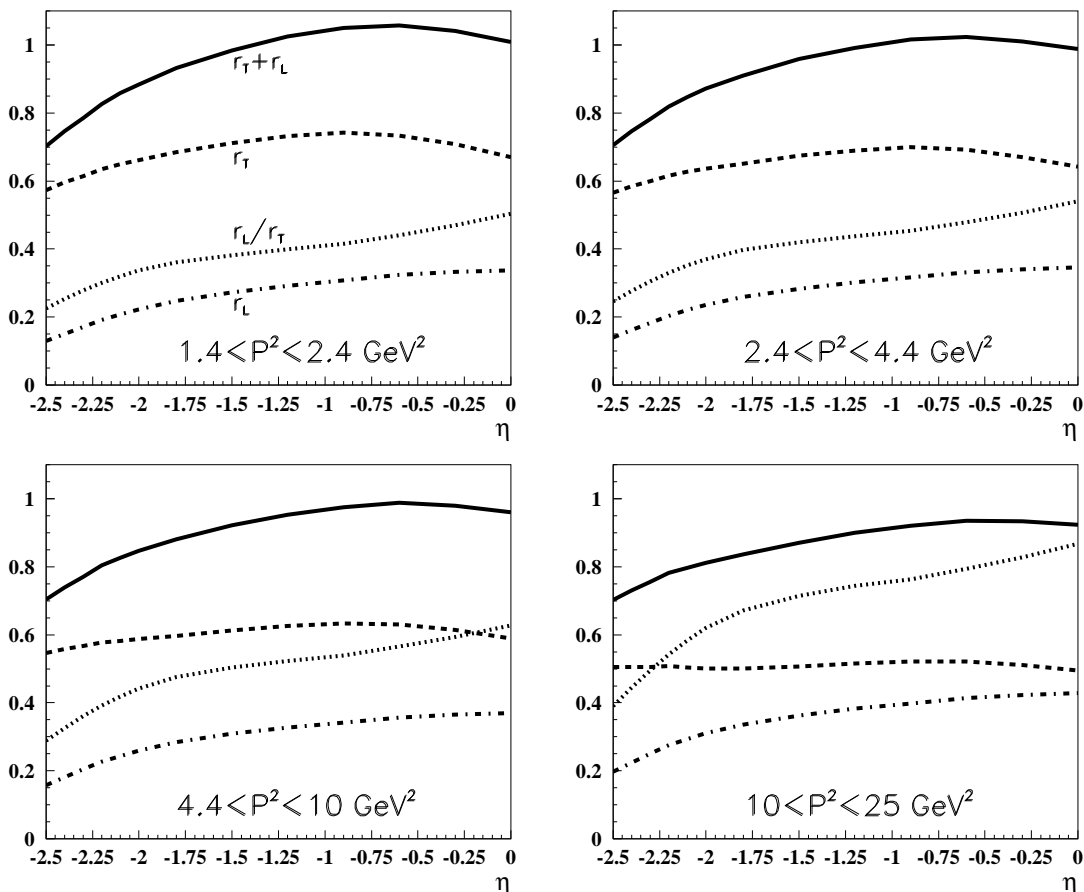


Figure 6: Fractional contributions  $r_L(\eta, P^2)$  and  $r_T(\eta, P^2)$  together with their sum and ratio.

$q_L^{\text{QED}} \otimes \sigma(\alpha_s^3)$ , which, similarly to those of  $\gamma_T^*$ , are not included in NLO  $\text{DIR}_{\text{uns}}$  calculations. However, as the current version of JETVIP takes into account in the resolved channel only the transverse virtual photons, they are not included even in the full  $\text{DIR}+\text{RES}$  calculations. The net nontrivial effect of introducing the concept of PDF of  $\gamma_L^*$  into JETVIP is then quantified by plotting in Fig. 7a the ratio

$$r_{\text{NLO}}(\eta, P^2) \equiv \frac{q_L^{\text{QED}} \otimes \sigma^{\text{res}}(\alpha_s^3)}{\sigma_{\text{DIR}+\text{RES}}}. \quad (17)$$

Also by this measure the contributions of  $\gamma_L^*$  are sizable. This net effect is much larger when the convolution  $q_L^{\text{QED}} \otimes \sigma^{\text{res}}(\alpha_s^3)$  is compared to the difference of  $\text{DIR}+\text{RES}$  and  $\text{DIR}_{\text{uns}}$  JETVIP results, measuring the nontrivial aspects of the concept of PDF of  $\gamma_T^*$  and corresponding to the gap between the thick solid and dashed curves in Fig. 5. As shown in Fig. 7b, the corresponding ratio, denoted  $r_{\text{nontriv}}(\eta, P^2)$ , is large, particularly for  $\eta$  close to lower edge  $\eta = -2.5$ .

## 4 How to measure partonic content of $\gamma_L^*$

In principle there is no obstacle to extracting partonic content of the virtual photon from experimental data by analyzing dijet production at two different values of  $y$ . This procedure is analogous to that involved in measuring the longitudinal structure function  $F_L^{\text{p}}(x, Q^2)$  of real hadrons, which requires performing the measurement at two different collisions energies. Although straightforward

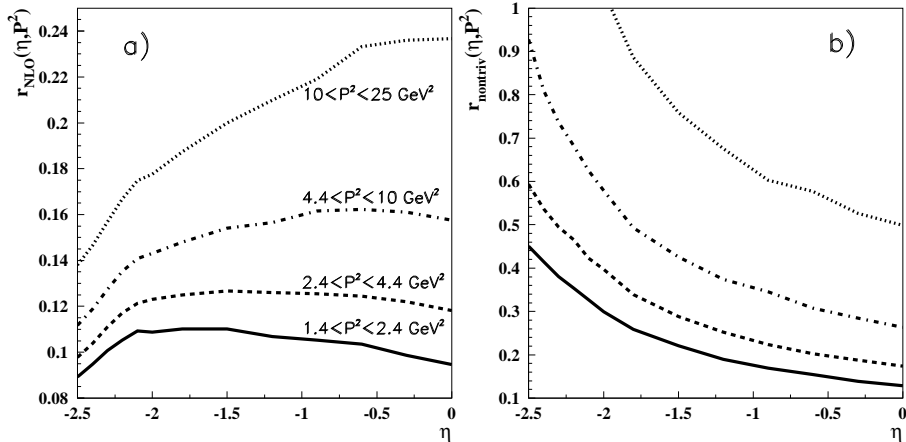


Figure 7: The ratio  $r_{\text{NLO}}(\eta, P^2)$  (defined in (16)) and  $r_{\text{nontriv}}(\eta, P^2)$  plotted as functions of  $\eta$ .

in principle, no such direct measurement of  $F_L^{\text{P}}$  has been performed at HERA, primarily for technical reasons related to changing the proton energy. For extraction of the partonic content of  $\gamma_L^*$  no such change of beam energies is necessary and it suffices to perform the analysis of dijet cross-sections at two different values of  $y$ . In practice, however, the separation of the contributions of  $\gamma_T^*$  and  $\gamma_L^*$  is not that simple, because it relies on different  $y$  dependencies of the corresponding fluxes (2-3) at large  $y$ . This in turn requires measuring jet cross-sections in narrow bins centered at two different values  $y_1$  and  $y_2$  instead of integrating over the whole interval of accessible  $y$ , which at HERA spans typically  $0.05 \lesssim y \lesssim 0.9$ . Optimizing the bin width and choice of the values  $y_1, y_2$  is crucial for the success of such extraction.

## 5 Summary and conclusions

We have demonstrated the importance of including in hard collisions the contributions of the longitudinal polarization of the target virtual photon. In QED these contributions are fully calculable and their onset is determined by the ratio  $P^2/m^2$  of photon virtuality  $P^2$  and fermion mass  $m^2$ . The inclusion of target  $\gamma_L^*$  is indispensable for good quantitative agreement of QED predictions with existing LEP data.

In QCD gluon radiation off the quarks or antiquarks coupling to  $\gamma_L^*$  is expected to modify simple QED formulae and, in addition, generate gluons inside  $\gamma_L^*$ . In this exploratory study we, nevertheless, neglected these effects and used the purely QED formula for quark distribution function of  $\gamma_L^*$ . The numerical relevance of  $\gamma_L^*$  has been illustrated within the framework of LO analysis of observables  $F_2^\gamma$  and  $D_{\text{eff}}$  as well as within the NLO calculations of dijet production at HERA. Better theoretical understanding of the structure of  $\gamma_L^*$  is, however, needed for more reliable evaluation of these effects.

**Acknowledgment:** We are grateful to J. Cvach, Ch. Friberg, B. Pötter, I. Schienbein and A. Valkárová for interesting discussions concerning the structure and interactions of longitudinal virtual photons. This work was supported in part by the Grant Agency of the Academy of Sciences of the Czech Republic under grants No. A1010821 and B1010005.

## References

- [1] Ch. Friberg, T. Sjöstrand, Eur. Phys. J. **C13** (2000), 151
- [2] M. Glück, E. Reya, I. Schienbein, Phys. Rev. **D60** (1999), 054019
- [3] V.M. Budnev, I.F. Ginzburg, G.V. Meledin, V.G. Serbo, Phys. Rep. **15C** (1975), 181
- [4] A. Gorski, B.L. Ioffe, A. Yu. Khodjamirian, A. Oganesian, Z. Phys. C **44**, 523 (1989)
- [5] J. Chýla, M. Taševský, Proc. *PHOTON '99*, Freiburg in Breisgau, May 1999, ed. S. Soeldner–Rembold, Nucl. Phys. B. Proc. Sup. 82 (2000), 49, hep-ph/9906552
- [6] J. Chýla, M. Taševský, Proc. *Monte–Carlo generators for HERA Physics*, Hamburg 1999, p. 239, hep-ph/9905444
- [7] J. Chýla, M. Taševský, hep-ph/9912245
- [8] B. Pötter, Comp. Phys. Comm. **119** (1999), 45, hep-ph/9806437  
G. Kramer, B. Pötter, Eur. Phys. J. **C5** (1998), 665, hep-ph/9804352
- [9] M. Acciari et al. (L3 Collab.), Phys. Lett. **B438** (1998), 363
- [10] G. Abbiendi et al. (OPAL Collab.), Eur. Phys. J. **C11** (1999), 409
- [11] J. Chýla: hep-ph/9911413
- [12] G. Schuler, T. Sjöstrand: Z. Phys. **C68** (1995), 607  
G. Schuler, T. Sjöstrand: Phys. Lett. **B376** (1996), 193
- [13] C. Adloff et al. (H1 Collab.), Eur. Phys. J. **C**, in print
- [14] M. Taševský, PhD Thesis, Charles University, Prague, unpublished
- [15] B. V. Combridge, C. J. Maxwell, Nucl. Phys. **B239** (1984), 429